

Mechanical properties and microstructure of hot rolled NM360/Q345R composite interface analysis

J. Li¹³, L.Ma^{123*}, G. Zhao¹²³, Q. Huang²³, X. Yang¹²³, M. Cheng¹²³

¹Taiyuan University of Science and Technology, Taiyuan 030024, Shanxi, China

²Shanxi Provincial Key Laboratory of Metallurgical Device Design Theory and Technology,

³The Coordinative Innovation Center of Taiyuan Heavy Machinery Equipment

Received August 18, 2017, Accepted December 18, 2017

The rolling reduction rate is one of the important factors that affect the bonded interface of a composite plate. In this paper, the mechanical properties and microstructure of the interface were studied for 30%, 50% and 70% rolling reduction rates. The NM360/Q345R composite plates were analyzed by a universal tensile testing machine, OM, SEM and EDS. As the rolling reduction rate increased, both the tensile strength and the elongation increased. When the reduction rates were 30% and 50%, the bonding interface was poor and apparent cracks could be observed after the tensile tests. When the reduction rate reached 70%, no voids or cracks existed, the breaking interface was smooth and neat and the bonding interface formed a common structure. Significant decarbonization of NM360 occurred at the bonding interface. When the reduction rates were 30% and 50%, long strips or black dots of particles appeared near the interface. The black particles were Mn and Si oxides, which could have a negative effect on the bonding interface.

Keywords: NM360/Q345R, Mechanical properties, Bonded interface, Microstructure.

INTRODUCTION

The wear-resistant composite steel plate is a new anti-wear composite material manufactured by a cladding technology, which could not only fully utilize the advantage of anti-wear alloys and base materials, but it could also make up for the corresponding shortcomings. Owing to their perfect performance not displayed by other single metals or alloys, the wear-resistant composite steel plates are widely utilized in various industrial fields [1-8].

The wear-resistant composite steel plates are often fabricated by an overlaying technology [9]. During overlaying, the base steel plate is unevenly heated; therefore the gradient of temperature fields is high. This could easily lead to high welding residual stress and deformation. Moreover, the overlaying leads to significant roughness of the overlaying surface, which could cause issues to further machining.

In hot roll bonding [10-12] rolling mills are utilized in the production of composite plates. As a result of the strong force of the rolling mill in combination with the thermal effect, two surfaces of compound metals are pressed together and plastic deformation occurs over the entire metallic cross-section [13].

Until recently, there have been only a few studies on wear-resistant hot rolled bonding plates has been significantly rare. Qiu [4] studied the effects of rolling and heat-treatment on the structure and properties of the NM450D/ Q235B clad plate [14]. Gong studied the cladding rolling technology of the wear-resistant steel/carbon steel [15].

In this paper, the mechanical properties, the metallographic structure and microstructure of the wear-resistant steel 360 (NM360) - carbon steel Q345R composite plate after vacuum hot rolling were analyzed.

EXPERIMENTAL PROCEDURE

Fabrication of hot-rolled two-layered NM360/Q345R composite

In this study, the two-layered NM360/Q345R composite was roll-bonded, Q345R, being the base layer and NM360 the cladding layer. The chemical composition of Q345R and NM360 is presented in Table 1.

Firstly, the NM360 and Q345R steels were prepared and underwent surface treatment. The composite surface had to be cleaned and smoothly ground, which allowed the two types of metal atoms to mutually diffuse and reach a metallurgical bonding.

Table 1. Main chemical composition of NM360 and Q345R materials (mass fraction %)

	C	Si	Mn	P	S	Cr	Ni	Mo	B
NM360	≤0.25	≤0.70	≤1.30	≤0.025	≤0.010	≤1.40	≤1.00	≤0.50	≤0.004
Q345R	0.15	0.35	1.40	0.013	0.004	—	—	—	—

By a wire brush machine the surfaces were polished until the "sand surface" effect was observed, though the surface roughness increase led to the subsequent rolled bonding of the composite. Subsequently, the polished surfaces were cleaned with absolute ethanol for surface adhesion and oil removal. The surfaces were blown-dried. Secondly, the NM360 and Q345R steels were batched and welded with the clean surfaces facing each other. The composite slab was sealed by argon arc welding and the vacuum evacuating nozzle was welded. Finally, a two-stage diffusion vacuum pump was utilized for the slab to be pumped to the high vacuum state of 1.0×10^{-3} Pa and the suction nozzle was sealed at a high temperature by hot pressure.

The NM360 thickness was 3 mm and the Q345R thickness was 10 mm. The NM360/Q345R composite slabs were preheated at 1200°C and held at this temperature for 10 min. Consequently, hot rolling experiments were performed at 0.2 m/s, the stacks were roll bonded with reduction rates of 30%, 50% and 70%, respectively and cooled down in the air, subsequently to rolling. The sizes of the stacks and the rolling conditions of hot rolled composite are presented in Table 2.

Microstructure analysis and mechanical tests

In order to evaluate the rolling reduction effects of the NM360/Q345R composites on the tensile strength, the rolled composites were prepared according to the Chinese Standard GB/T 6396-2008, along the rolling direction. For the tensile fracture type study, the tensile fracture surfaces were observed by a scanning electron microscope (SEM).

The NM360/Q345R composites were polished and etched in a solution of 4% nitric acid and 96%

ethyl alcohol. The RD-ND plane microstructure was observed by ultra-deep microscope (OM), scanning electron microscope (SEM) (ZEISS SIGMA FE-SEM) and EDS.

RESULTS AND DISCUSSION

Mechanical properties of NM360/Q345R composite plate

Fig.1 demonstrates the tensile strength data of the NM360/Q345R composites with various rolling reduction rates. The yield and tensile strength increased along with the elongation, as the rolling reduction rate increased. Regarding the NM360/Q345R composite at 70% rolling reduction rate, the yield and tensile strength reached the maximum of 396.12 MPa and 514.84 MPa respectively, whereas the elongation was the longest, 39.95%. The tensile strength revealed that coherent and well-bonded layers could support each other; this had a direct effect on both the tensile strength and the elongation [16]. The best performance was observed when the reduction rate was 70%.

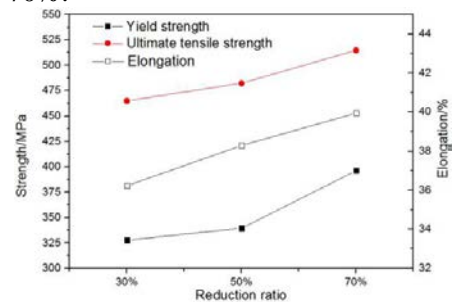


Fig.1. Comparison of mechanical properties of NM360/Q345R composite

Tensile fractography

Fig. 2 a/b presents the fractography at 30% and 50% reduction rate, respectively.

Table 2. Various base layer thicknesses of rolling compound crafts

	Plate length +width	NM360	Q345	Rolling temperature	Rolling reduction rate
1	200×100	3mm	9mm	1150°C	30%
2	200×100	3mm	9mm	1150°C	50%
3	200×100	3mm	9mm	1150°C	70%

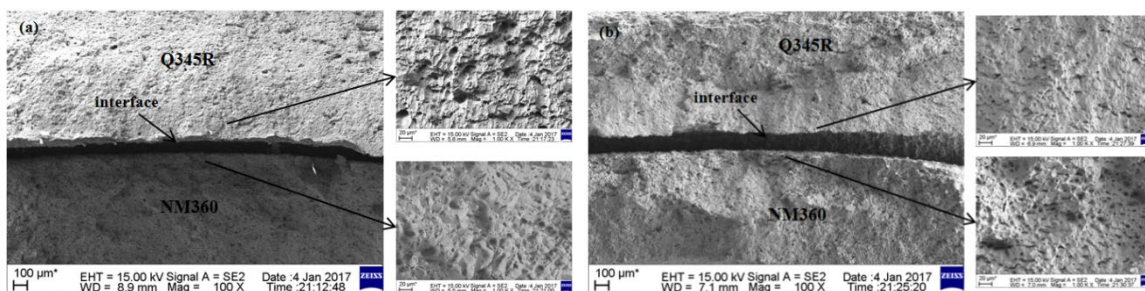


Fig. 2. Interface and fracture morphology of NM360/Q345R composite: (a) 30% reduction rate; (b) 50% reduction rate

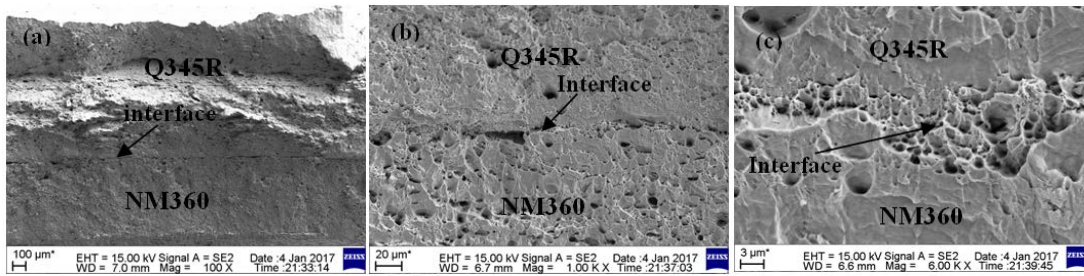


Fig. 3. Interface and fracture morphology for NM360/Q345R composite at 70% reduction rate

Subsequently to tensile failure, an apparent delamination could be observed from the low-magnification picture (100 \times) in these two conditions, which could be attributed to low bonded strength and poor compatibility of deformation. In NM360 and Q345R a high number of dimples existed, therefore it could be proved that the fracture type of the substrates was ductile. As the reduction rate increased, an increasing number of dimples on the substrates occurred and became increasingly low-sized. It could be observed that the toughness of every single layer was improved as the reduction rate increased, which could also be proved from the tensile mechanical properties.

Fig. 3 presents the tensile fracture morphology at 70% reduction rate. The bonding interface was quite straight and neat, no visible cracks and high-sized pores appeared which proved that the bonding performance was good, as shown in Fig. 3a/b. When the reduction rate increased to 70%, the interface was well-bonded and no delamination could be observed at the interface. Therefore, the bonding strength was high. Through further observation of the fracture morphology (Fig. 3b/c), it could be seen that the substrates near the interface displayed a number of dimples that were the typical ductile fracture feature, demonstrating that a ductile fracture occurred on the substrate. Compared to Q345R or te NM360, the dimples on the interface were quite close and the overall interface was well combined. From the aforementioned discussion, only at a reduction rate of 70%, good bonding

between NM360 and Q345R could be obtained under the tested conditions.

Microstructure analysis of interface

The microstructure morphology and grain size under various reduction rates were analyzed by OM. It could be observed that the bonding interface was straight and the NM360 grain size exceeded the Q345R grain size. Defects such as holes in the composite interface were not observed and the grain distribution was uniform, which indicated that a bonded interface could be formed under the experimental conditions. The Q345R side formed a high amount of pearlites that are displayed as black bands in Fig. 4. Also, as the rolling pressure increased, the pearlites changed from coarse to fine.

A degree of decarburization existed on the side of NM360. This was due to the fact that the mass fraction of NM360 exceeded that of Q345R and the carbon atoms of the NM360 side spread to the Q345R side. It was observed that the carbon steel side decarburizing layer width decreased as the reduction rate increased. Although the high temperature could beneficiate carbon atoms diffusion, the deformation effect on the decarburization layer was higher compared to the temperature effect. Therefore, the decarburization layer became thin when the rolling pressure gradually increased. In addition, the grain size became increasingly lower as the reduction rate increased, which was due to the occurrence of total recrystallization in the grains. This recrystallization could make the grains fine and improve the mechanical behavior of the composite plate.

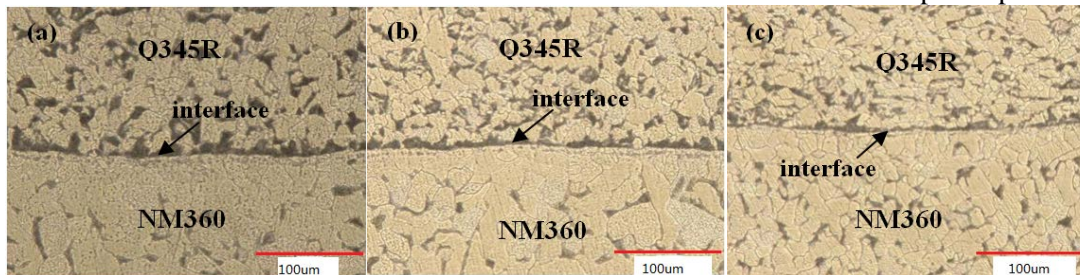


Figure.4. OM of NM360/Q345R composite (a) 30% reduction rate; (b) 50% reduction rate; (b) 70% reduction rate

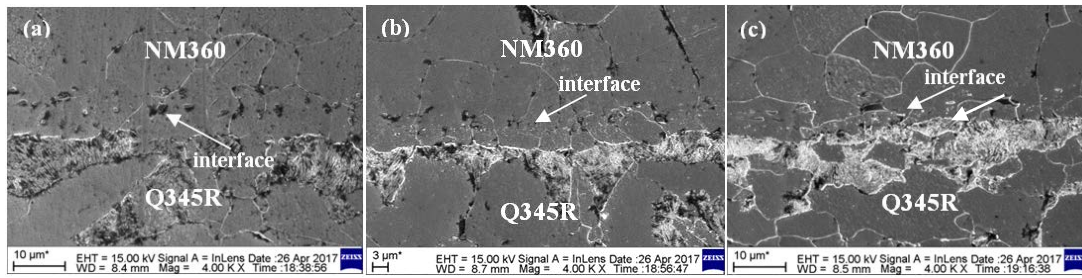


Fig.5. SEM of NM360/Q345R composite: (a) 30% reduction rate; (b) 50% reduction rate; (b) 70% reduction rate

The SEM micrographs of the NM360/Q345R are presented in Fig. 5a/c. The material interfaces were bonded without pores or voids, which indicated a successful fabrication of NM360/Q345R sheets by hot-roll-bonding. Thin elongated pearlites were located along the interface. The NM360/Q345R composite plate structures were mainly ferrite and pearlite. The mechanical performance was defined by the pearlite spacing and the pearlite mass diameter, because fracture usually occurred on the surfaces of pearlite and ferrite when the lamellar pearlite was being stretched by external forces. When the pearlite spacing and mass diameter became low, the phase interface increased and the dislocation motion inhibition was high. This led to an increase in the deformation resistance and possibly contributed to the strength, hardness and plasticity improvement. Moreover, the lamellar pearlite spacing decreased. When the carburizing layer was significantly thin, it could slide under external force, possibly producing plastic deformation and also be bent. As the rolling reduction rate increased, both the spacing and the diameter of pearlite in the NM360/Q345R composite interface decreased, which could improve the mechanical properties. When the reduction rate reached up to 70%, lowest pearlite spacing and pearlite mass spacing diameter were observed. This ensured that the composite interface was well combined and was not stratified during stretching (as shown in Fig. 6).

The transformation of pearlite included an incubation period, the carbide nucleus grew along with the iron grain core growth. During pearlite

transformation, the strong carbide forming elements titanium, niobium and vanadium formed alloy carbides, while the weak carbide forming element manganese formed rich manganese alloy cementite. Therefore, the nucleation and growth of carbides depended on the diffusion and enrichment of the elements. The atomic diffusion coefficient of the carbide forming element in austenite was by 10^5 orders of magnitude slower than the atomic diffusion coefficient of the carbon atom, which could slow down the nucleation and growth of the alloy carbide or cementite and lead to an increase in the pearlite transformation period, whereas the pearlite spacing decreased [17]. Significantly low amounts of manganese existed at the interface, which means that the micro-alloy addition to steel could not only have an effect on the refined grain and precipitation strengthening. Also, the carbide formed by the micro-alloy elements could refine the pearlite lamellar spacing and further improve the strengthening effect. As the reduction rate increased, the NM360/Q345R recrystallization well refined the austenitic grains. Moreover, elements such as Mn and Si, dispersed in the interface, provided conditions for a high amount of pearlite to be formed. The composite plate thermal deformation temperature decreased as the rate increased, which could reduce the carbide forming elements atomic diffusion coefficient in austenite, further leading to a significant slow down of nucleation and growth of the alloy carbide or alloying cementite. This phenomenon increased the incubation period of pearlitic transformation and decreased the pearlite spacing.

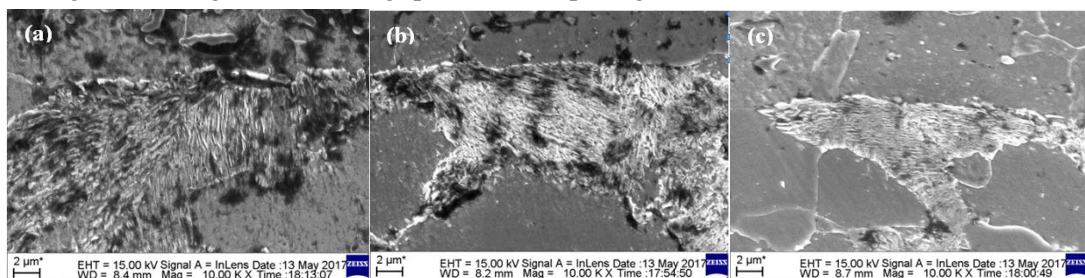


Fig. 6. SEM of pearlite at the interface of NM360/Q345R composite: (a) 30% reduction rate; (b) 50% reduction rate; (b) 70% reduction rate

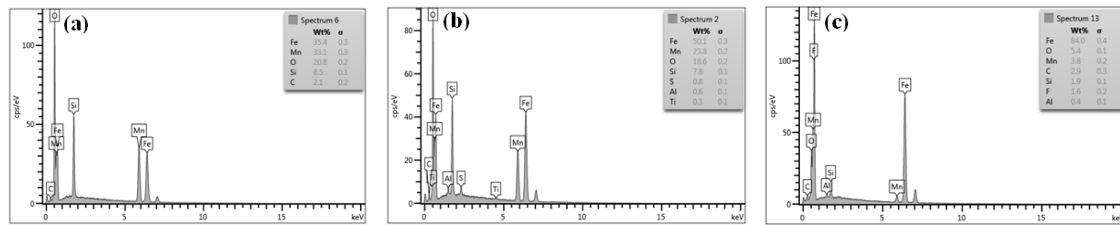


Fig.7. EDS of particles at interface of NM360/Q345R composite: (a) 30% reduction rate; (b) 50% reduction rate; (c) 70% reduction rate

Through further observation, the interface had a continuous dense distribution of dotted black particles or black long strips, when the reduction rate was low. The interface had a high amount of oxygen by point scanning (Fig. 7), even if the NM360/Q345R slab was vacuumed. Since the surface to be bonded was rough, a high amount of oxygen was still attached to the surface. Except oxygen, there were also Fe, Mn and Si. Fe is an inherent element in both NM360 and Q345R, whereas Mn and Si were elements in NM360 and Q345R that were diffused around the interface. It was found that the black objects at the interface were Mn and Si oxides and these oxides had an effect on the bonding strength. Also, similar studies demonstrated that both black impurities and oxides formed at the interface. Nomura *et al.* [18] discovered that a steel surface containing Si and Mn was easy to produce Si-Mn oxide formations [18]. Peng *et al.* [19] reported that the breakdown oxide led both sides of the interface to reach a solid metallurgical combination during rolling[19]. The higher the amount of fine oxides, the easier was the interface bonding. Jing *et al.* [20] reported that a 5 μm wide black strip inclusion existed at the interface of the steel/carbon steel composite, which was caused by both oxidation and diffusion [20].

Therefore, when the reduction was 30% and 50%, the mechanical properties of the composite were poor and cracks occurred through stretching. As presented in Fig. 8, the long strips of particles became lower-sized and distributed in the interface, which occurred because the oxide was crushed under the high positive pressure. When the reduction rate increased to 70%, no black particles existed. The crushed oxide was dissolved in the structure of the bonding interface and subsequently dispersed in the interface, leading to low impact on the interface. Therefore, at a higher roll reduction rate, the interface was significantly improved.

CONCLUSIONS

In this paper, the effects of rolling reduction rates on the mechanical properties, metallographic interface and microstructure of the NM360/Q345R composite were studied.

1) As the rolling reduction rate increased, both the tensile strength and the elongation increased. The best comprehensive performance occurred when the reduction rate was 70%.

2) At a reduction rate of 30% and 50%, the bonding interface was poor and apparent cracks could be observed subsequently to the tensile tests. When the reduction rate reached up to 70%, no voids or cracks existed and the breaking interface was smooth and neat. Also, the bonding interface formed a common structure.

3) It could be observed by the ultra-deep microscope that the bonding interface was straight. Significant decarbonization of NM360 occurred. When the reduction rate was 30% and 50%, long strips or black dotted particles appeared near the interface. These black particles were Mn and Si oxides, which could have a negative effect on the bonding interface.

Acknowledgements: This project was supported by the Coordinative Innovation Center of Taiyuan Heavy Machinery Equipment, the Joint Funds of the Coal Based and Low Carbon of Shanxi(U1510131), the Foundation for Young SanJin Scholars of Shanxi, the Key Research and Development Program of Shanxi Province(201603D111004 and 201603D121010), the Science and Technology Major Project of Shanxi Province(MC2016-01), and the Collaborative Innovation Center of Taiyuan Heavy Machinery Equipment.

REFERENCES

1. Z. Yang, Z. Meng, *Metallurgical Equipment*, **6** (3), 55 (1997).
2. R.C. Schrama, *Lubrication Engineering*, **50** (6), 438 (1994).
3. X.Wen, X. Wang, X. Yuan, P. Wwn, Q. Yang, *Heat Treatment*, **26** (3), 56 (2011).
4. X.W. Qiu, Y.P. Zhang, G.L. Chun, *Applied Mechanics and Materials*, **121-126**, 3551-3554(2012).
5. F.C. Li, *Shandong University of Science and Technology* (2011).
6. L.G. Zhang, *Cement Engineering*, (3),50-53(2012)
7. Yuan Jinsheng, *China Building Material Equipment*, (3), 26-27(1996).
8. P. Zhang, Y.H. Zhang, Q.M. Chang, *Foundry Equipment and Technology*, **2**(1),53-55 (2012)

9. L. Li, M.Y. Chen, *Wide and heavy plate*, **22**(2),38-43 (2016)
10. J.Y. Kang, J.G. Kim, S.K. Kim, K.G. Chin, S. Lee, H.S. Kim. *Scripta Materialia*, **123**,122-125 (2016)
11. J. Park, M. Kang, S. S. Sohn, J. S. Kim, H. S. Kim, W. T. Cho, *Materials Science & Engineering A*, **686**,160-167, (2017).
12. J. Park, J.S. Kim, M. Kang, S.S. Sohn, W.T. Cho, H.S. Kim, *Scientific Reports*, **7**:40231,(2017).
13. G. Zhao, Q. Huang, C. Zhou, Z. Zhang, L. Ma, X. Wang, *Revista De Metalurgia* , **52**(2), e069, (2016).
14. J. Qiu, X.R. Cheng, K. Lan, D. Lei, D.J. Huang, *Special Steel*, (2),56-59(2017)
15. C.W. Gong, *Wuhan University of Science and Technology* (2015).
16. R. Abedi, A. Akbarzadeh, *Materials & Design*, **88**, 880-888 (2015).
17. C. Yang, *Kunming University of Science and Technology* (2011).
18. M. Nomura, I. Hashimoto, S. Kozuma, M. Kamura, Y. Omiya, *Tetsu-to-Hagane*, **92**(6), 378-384(2006)
19. X.K. Peng, R. Wuhler, G. Heness, W.Y. Yeung, *Journal of Materials Science*, **35**(17),4357-4363 (2000)
20. C. Jing, J. Tong, Beijing, *Journal of University of Science & Technology Beijing*, **29**(10), 985-988.(2007)